JACS
JOURNAL OF THE AMERICAN CHEMICAL SOCIETY

ARTICLE

pubs.acs.org/JACS

Bacterial Toxin-Triggered Drug Release from Gold Nanoparticle-Stabilized Liposomes for the Treatment of Bacterial Infection

Dissaya Pornpattananangkul,[†] Li Zhang,[‡] Sage Olson,[†] Santosh Aryal,[‡] Marygorret Obonyo,[§] Kenneth Vecchio,[‡] Chun-Ming Huang,[∥] and Liangfang Zhang*[,‡,⊥]

[†]Department of Bioengineering

[‡]Department of NanoEngineering

[§]Division of Infectious Diseases

[∥]Division of Dermatology

[⊥] Moores Cancer Center

University of California San Diego, La Jolla, California 92093, United States

ABSTRACT: We report a new approach to selectively deliver antimicrobials to the sites of bacterial infections by utilizing bacterial toxins to activate drug release from gold nanoparticle-stabilized phospholipid liposomes. The binding of chitosan-modified gold nanoparticles to the surface of liposomes can effectively prevent them from fusing with one another and from undesirable payload release in regular storage or physiological environments. However, once these protected liposomes "see" bacteria that secrete toxins, the toxins will insert into the liposome membranes and form pores, through which the encapsulated therapeutic agents are released. The released drugs subsequently impose antimicrobial effects on the toxin-secreting bacteria. Using methicillin-resistant *Staphylococcus aureus* (MRSA) as a model bacterium and vancomycin as a model anti-MRSA antibiotic, we demonstrate that the synthesized gold nanoparticle-stabilized liposomes can completely release the encapsulated vancomycin within 24 h in the presence of MRSA bacteria and lead to inhibition of MRSA growth as effective as an equal amount of vancomycin-loaded liposomes (without nanoparticle stabilizers) and free vancomycin. This bacterial toxin enabled drug release from nanoparticle-stabilized liposomes provides a new, safe, and effective approach for the treatment of bacterial infections. This technique can be broadly applied to treat a variety of infections caused by bacteria that secrete pore-forming toxins.

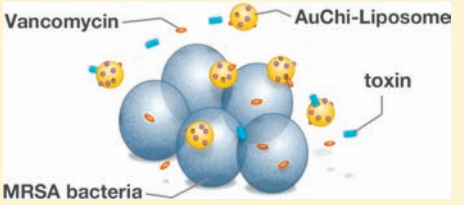

INTRODUCTION

Using nanoparticles to differentially deliver therapeutic agents to the sites of action (also called targeted drug delivery) represents a central goal, a key challenge as well, of nanomedicine research.[1−3] A common approach to reach this goal is to functionalize the surface of the nanoparticles with targeting ligands that specifically bind to the receptors overexpressed by the target cells.[4,5] Various molecules have been demonstrated to bind to target cells, including antibodies, antibody fragments, aptamers, peptides, small molecules, and so on.[6,7] While great progress has been made to use ligands for active cellular targeting, none of the products have ever been approved, and only three targeted nanoparticle systems are now in phase I/II clinical trials.[4,8] This is mainly due to the complexity and the off-target effect of these ligand-modified nanoparticles. Herein we report an entirely new concept of targeted drug delivery to treat bacterial infections. Instead of using targeting ligands to actively target the drug carriers to the bacteria of interest, we take advantage of the biomolecules, such as toxins, secreted by the target bacteria and use them to trigger the release of therapeutic payloads and thus kill the bacteria. In this approach, prior to seeing the target bacteria, drugs are protected inside the nanocarriers and will not be released, thereby eliminating all adverse side effects due to premature drug leakage or nonspecific drug release. As a proof-of-concept, here we demonstrate that bacterial toxins can be utilized to trigger antibiotic release from gold nanoparticle-stabilized phospholipid liposomes and that the released antibiotics can subsequently inhibit the growth of *Staphylococcus aureus* (*S. aureus*) bacteria that secrete the toxins.

This study intends to integrate the therapeutic needs to treat bacterial infections with the well-studied pore-forming activities of toxins secreted by bacteria and the recent advancements in liposome chemistry. There are a variety of molecules that possess pore-forming activity, including bacterial toxins, animal toxins, immune proteins, and synthetic compounds, such as Triton X-100.[9−12] Alpha hemolysin, also named α-toxin, is one of the common toxins secreted by *S. aureus* bacteria as a water-soluble protein monomer with a molecular weight of 34 kDa.[13] This protein can spontaneously incorporate into lipid membranes and self-oligomerize to form a heptameric structure with a central pore. The pore size is about 2 nm that allows small molecules up

Received: December 10, 2010
Published: February 23, 2011

dx.doi.org/10.1021/ja111110e | *J. Am. Chem. Soc.* 2011, 133, 4132–4139

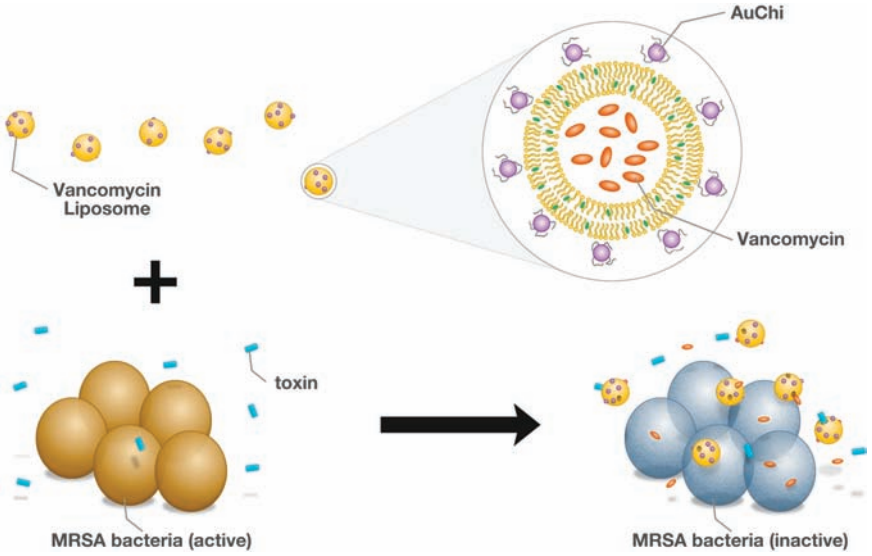

Figure 1. Schematic principle of bacterial toxin-triggered antibiotic release from gold nanoparticle-stabilized liposomes to treat toxin-secreting bacteria. Vancomycin-loaded liposomes are protected by absorbing chitosan-coated gold nanoparticles (AuChi) onto their surface to prevent them from fusing with one another or with bacterial membranes. Once the AuChi-stabilized liposomes (AuChi-liposome) encounter bacterial toxins, the toxins will form pores in the liposome membranes and thus release the encapsulated antibiotics, which subsequently kill or inhibit the growth of the bacteria that secrete the toxins.

to 3 KDa to passively diffuse through the membranes.[14,15] In nature, *S. aureus* bacteria secrete α-toxin that can bind to the outer membranes of susceptible cells. Upon binding, rapid pore-forming facilitates uncontrolled permeation of water, ions, and small molecules, rapid discharge of vital molecules, such as ATP, dissipation of the membrane potential and ionic gradients, and irreversible osmotic swelling leading to the cell lysis.[13] Considering the tremendous availability of bacterial toxins at bacterial infection sites and their pore-forming activities, we hypothesize that these invasive molecules can be utilized to selectively release antimicrobials from liposomes that are stabilized by small gold nanoparticles to avoid undesirable membrane−membrane fusion and drug leakage. This strategy allows smart release of drugs at the infectious sites to kill toxin-secreting bacteria while not producing any toxic effects on healthy tissues.

Liposomes are spherical lipid vesicles with a bilayer membrane structure consisting of amphiphilic lipid molecules and have been studied extensively as antimicrobial drug delivery vehicles for decades due to their unique features, including highly biocompatible lipid materials, ability to deliver hydrophilic and lipophilic drugs, lipid bilayer structure that can fuse with bacterial membranes, and easy surface modification.[16−18] There are a few liposome formulations that have been approved by the Food and Drug Administration (FDA) for therapeutic purposes. For example, AmBisome (NeXstar Pharmaceuticals, San Dimas, CA) is an FDA approved liposomal formulation of amphotericin B, which has been widely used in the clinic to treat *Candida* spp, *Aspergillus* spp, *Fusarium* spp, and other fungi infections in neutropenic, visceral leishmaniasis, and methylmalonic acidaemia patients.[19,20] Despite these advantageous features of liposomes as a delivery vehicle, the applications of liposomes are usually limited by their instability due to uncontrollable fusion among liposomes, leading to short shelf life, undesirable payload loss, and unexpected mixing.[21−23] An extensively used approach to stabilize liposomes is to coat their surface with a "stealth" material such as polyethylene glycol (PEG).[24,25] PEGylated liposomes can not only prevent liposomes from fusing with one another but also enhance their in vivo circulation lifetime by suppressing plasma proteins from adsorbing onto the liposome surface. Therefore, they have been widely used for systemic drug delivery.[26] However, PEGylated liposomes are rarely used for topical drug delivery, especially to treat bacterial infections. This is mainly because the polymer coatings will not only stabilize liposomes against fusion but also prevent them from fusing with bacterial membranes or prevent pore-forming proteins, such as toxins, from accessing to the liposomes to release drug payloads. Therefore it would be desirable to develop liposomes that are stabilized against fusion with synthetic or biological membranes, but they are accessible to pore-forming proteins for controlled drug release, once they are applied onto the target skin sites.

Recently, Granick et al. have reported a unique approach to stabilize liposomes against fusion with one another by adsorbing either anionic or cationic nanoparticles onto liposomal surfaces.[27−29] This strategy has effectively improved liposome stability; however, drug release from these nanoparticle-stabilized liposomes is greatly inhibited due to the relatively rigid membrane upon nanoparticle attachment. We recently reported an acid-responsive approach to resume liposome fusion activity and then release the encapsulated drugs at the sites of action.[30] This method is based on the surface charge profile change of carboxyl-modified gold nanoparticles in response to environmental acidity and allows to selectively deliver liposomal drugs to tissues at acidic condition where pH < 5.

Herein, we synthesize a novel liposome formulation stabilized by chitosan-modified gold nanoparticles (AuChi) to differentially release a model antibiotic, vancomycin, to inhibit the growth of *S. aureus* bacteria for topical treatment of skin bacterial infections. Figure 1 illustrates the working principle of toxin-triggered antibiotic release from gold nanoparticle-stabilized liposomes for the treatment of the bacteria that secrete the toxins. The cationic AuChi bind to the negatively charged liposome surfaces through electrostatic attraction and thus

stabilize liposomes against fusion with one another and avoid undesirable antibiotic leakage. When the stabilized liposomes are in the vicinity of *S. aureus* bacteria, the bacterium-secreted toxins will insert into the liposome membrane and create pores, through which the encapsulated antibiotic will be released. The released vancomycin, as staying in close to the bacteria, will then exert its antimicrobial activity rapidly and locally. In the study, we test the pore-forming activity and payload release kinetics of the AuChi-stabilized liposomes (AuChi-liposome) in the presence of α-toxin and *S. aureus* bacteria, respectively. We also demonstrate that the released antibiotics from the liposomes in the presence of *S. aureus* are sufficient to inhibit the growth of the bacteria.

EXPERIMENTAL SECTIONS

Materials. Hydrogenated L-α-phosphatidylcholine (Egg PC) and cholesterol were purchased from Avanti Polar Lipids, Inc. (Alabaster, AL). Sephadex G-75 was purchased from Fisher Scientific (Pittsburgh, PA), and 8-aminonaphthalene-1,3,6-trisulfonic acid disodium salt (ANTS) and *p*-xylene-bis-pyridinium bromide (DPX) were obtained from Invitrogen (Carlsbad, CA). Poly(ethylene glycol) methyl (M_n = 2000 Da) and triptic soy broth (TSB) were purchased from Sigma Aldrich (St Louis, MO). Hydrogen tetrachloroaurate ($HAuCl_4$) and sodium borohydride ($NaBH_4$) were from ACROS Organics (Geel, Belgium). Chitosan-50 was purchased from Wako Pure Chemical Industries, Ltd. (Osaka, Japan).

Preparation and Characterization of AuChi and AuChi-Liposome. AuChi were prepared by a sodium borohydride reduction technique.[30,31] Briefly, aqueous solution of $HAuCl_4$ (10^{-4} M, 50 mL) was reduced by 0.005 g of $NaBH_4$ at ice cold temperature to prepare bare gold nanoparticles. The acquired bare gold nanoparticles were then incubated overnight with 0.1% w/v chitosan that was predissolved in 0.1 M acetic acid. The resulting AuChi were purified three times by an Amicon Ultra-4 centrifugal filter with a molecular weight cutoff of 10 kDa (Millipore, Billerica, MA).

Liopsomes were prepared following a previously described extrusion method.[32] Briefly, 9 mg of lipid components were dissolved in 1 mL chloroform, and then the organic solvent was evaporated by blowing argon gas over the solution for 15 min to form a dried lipid film. The lipid film was rehydrated with 3 mL of deionized water or PBS with ANTS/DPX dyes or vancomycin, followed by vortexing for 1 min and sonicating for 3 min in a bath sonicator (Fisher Scientific FS30D, Pittsburgh, PA) to produce multilamellar vesicles (MLVs). Then the obtained MLVs were sonicated for 1−2 min at 20 W by a Ti probe (Branson 450 sonifier, Danbury, CT) to produce unilamellar vesicles. The solution was extruded through a 100 nm pore-sized polycarbonate membrane for 11 times to form narrowly distributed small unilamellar vesicles (SUVs). The liposomes were purified by gel filtration with a Sephadex G-75 column equilibrated with water or isotonic PBS solution to remove unencapsulated dyes or drugs. To prepare AuChi-liposome, the pH of both AuChi and liposome solutions was adjusted to 6.5 using HCl. Then the liposomes and AuChi at desired molar ratio were mixed together, followed by 10 min bath sonication.

UV−vis absorbance spectrum of AuChi from 300 to 600 nm was recorded by a spectrophotometer (Infinite M200, TECAN, Männedorf, Switzerland). The morphology of the AuChi was characterized by a scanning transmission electron microscope (STEM) equipped with a cold cathode field emission electron source and a turbo-pumped main chamber (Hitachi HD2000, Tokyo, Japan). The STEM was operated at 200 keV accelerating voltage and 20 mA current, and images were recorded in both secondary electron mode and transmitted electron mode. Elemental analysis was performed with an EDAX energy dispersive X-ray spectrometer (EDS). Malvern Zetasizer ZS (Malvern Instruments, Worcestershire, UK) was used to measure the hydrodynamic size and surface ζ potential of the prepared AuChi, liposome, and AuChi-liposome. The mean liposome diameter and surface ζ potential were determined by dynamic light scattering (DLS) and electrophoretic mobility measurements, respectively. All characterization measurements were repeated three times at 25 °C.

AuChi-Liposome Stability. Liposomes, loaded with 12.5 mM of ANTS and 45 mM of DPX, were mixed with AuChi at different molar ratios (1:0, 1:150, or 1:300). The obtained AuChi-liposome was incubated with bare liposomes, which were neither loaded with dyes nor stabilized by AuChi, at a molar ratio of 1:4 for 1 h at room temperature. The samples were then filtered through a Microcon YM-100 centrifugal filter with a molecular weight cutoff of 100 kDa (Millipore, Billerica, MA) for 20 min at 13.2×10^3 rpm. The amount of ANTS in the filtrate was measured for its fluorescence emission intensity at 510 nm using a fluorescent spectrophotometer (Infinite M200, TECAN, Männedorf, Switzerland) with an excitation wavelength of 360 nm.

Pore Forming Assay. To study the pore-forming activity of α-toxin against liposomes, 12.5 mM of ANTS and 45 mM of DPX were coencapsulated into the liposomes, at which the fluorescence of ANTS was maximally quenched by DPX. The resulting liposomes (600 μg/mL) were then incubated with α-toxin (20 μg/mL) for 1 h at room temperature. Once the pore forms, the encapsulated dyes will leach out of the liposomes, resulting in a florescence recovery of ANTS. After incubation, the fluorescence emission intensity of ANTS at 510 nm was measured by using a fluorescent spectrophotometer with an excitation at 360 nm. To obtain maximal dye leakage, Triton X-100 (1% v/v) was used as a positive control to completely lyse the liposomes. ANTS/DPX-loaded liposomes at the corresponding concentrations in the absence of α-toxin served as a negative control and experimental background. To determine the optimal liposome formulation, liposomes composed of Egg PC and cholesterol (0, 10, 25, and 50 wt %) were prepared and loaded with ANTS/DPX dyes to test their pore-forming property, respectively. The effect of PEG on liposome pore-forming property was assessed by adding PEG into the liposome solutions at various PEG concentrations: 1, 25, 50, 100, or 150 mg/mL.

Toxin-Triggered Vancomycin Release. Vancomycin-loaded (10 mg/mL) liposomes were stabilized by AuChi (vancomycin AuChi-liposome). To measure the drug loading yield of vancomycin liposome and vancomycin AuChi-liposome, 1 mL of the liposome solution was vacuum dried for 2 h to remove all the liquid, and the pallet was then reconstituted with 500 μL water. The obtained suspension was centrifuged at 5000 rpm for 5 min, and the supernatant was collected for reversed phase high-performance liquid chromatography (HPLC) using Agilent 1100 series (Santa Clara, CA). Samples were injected into a Zorbax C_{18} column with an injection volume of 80 μL. The elution was performed with a gradient mobile phase composed of acetonitrile and water with 0.1% (v/v) trifluoroacetic acid (TFA) (8−18% acetonitrile, 0−20 min) at a flow rate of 1 mL/min. Vancomycin was detected by a UV−vis detector at 280 nm, and the detector temperature was 20 °C. The acquired vancomycin intensity was compared with a linear standard curve of vancomycin at different concentrations to calculate the amount of vancomycin encapsulated inside the liposomal formulations.

To measure the toxin-triggered vancomycin release from the liposomes, the sample was mixed with PEG (100 mg/mL) and incubated with a methicillin-resistant *S. aureus* strain, MRSA252 (1×10^8 CFU/mL), in 5% (v/v) TSB at 37 °C for 0.5 and 24 h, respectively. After incubation, free vancomycin was separated by filtration through centrifugal filter unit (100 kDa MWCO) for 20 min at 13.2×10^3 rpm. The amount of vancomycin in filtrate was quantified by HPLC following the protocol described above.

Antimicrobial Assay. Vancomycin AuChi-liposome was mixed with PEG (100 mg/mL) and incubated with MRSA252 (1×10^8 CFU/mL) in 5% (v/v) TSB at 37 °C for 24 h. After incubation, the absorbance of the bacteria at 600 nm was measured by a spectrophotometer to determine bacterial growth. To exclude possible interference from background, the absorbance of the corresponding samples without MRSA252 was measured and subtracted from the obtained OD_{600}. In the study, vancomycin-loaded liposome without AuChi stabilization (vancomycin liposome) and free vacomycin served as positive controls, while AuChi-liposome (without vancomycin) and PBS served as negative controls. All experiments were repeated three times.

RESULTS AND DISCUSSION

In order to prepare AuChi-liposome, AuChi were first synthesized by an ex situ stabilization technique following a previously described protocol.[30,31] Briefly, gold hydrosol was synthesized by sodium borohydride reduction method and then was stabilized by a calculated amount of chitosan in an ambient condition. The formation of AuChi was first confirmed by the ^{1}H NMR spectroscopy. As shown in Figure 2A, the characteristic proton resonance of chitosan was significantly shifted toward upfield when chitosan was attached to gold nanoparticles. For example, in the spectrum of free chitosan, the protons at α-carbon (anomeric carbon, C-1) with a resonance peak at 4.8 ppm was completely masked by the broad D_2O resonance; the protons at β-carbon (C-2 carbon) showed a resonance peak at 2.9 ppm; and all other glycosidic protons were centered at 3.3−3.8 ppm. In contrast, in the ^{1}H NMR spectrum of AuChi, both α and β protons were shifted from 4.8 to 4.3 ppm and 2.9 to 2.5 ppm, respectively. In addition, the broad peaks centered at 3.3−3.8 ppm corresponding to the glycosidic protons of chitosan were significantly shifted toward upfield and centered at 2.6 to 3.5 ppm. This significant shifting of protons toward upfield can be attributed to their close proximity to the metal center and the inhomogeneity created by metal center, which further confirms the formation of AuChi. Similar shifting of proton resonance in close proximity to the metal center has been previously observed on different amino acid capped gold nanoparticles.[31] The formation of AuChi was further confirmed by UV−vis spectroscopy. As shown in Figure 2B, AuChi exhibited a strong absorbance at 512 nm, characteristic of the corresponding bare gold nanoparticles without chitosan coating. This indicates that the coating of chitosan did not alter the plasmon resonance of gold nanoparticles. The morphology of the AuChi particles was imaged by STEM. Secondary electron (SE) signal, which provides surface topology detail, showed ~10 nm size of AuChi with nearly uniform size distribution. The direct transmitted electron (TE) signal showed ~4 nm size of the inner gold core, which was consistent with the size of unmodified gold nanoparticles. Based on both the SE and TE images (Figure 2B insets), we conclude that the increase in size from 4 to 10 nm was solely contributed by the coating of chitosan but not the aggregation of gold particles.

As surface properties of AuChi are crucial for their interactions with liposomes, we next characterized the surface ζ potential of AuChi by measuring their electrophoretic mobility using DLS. The ζ potential of AuChi was 43.4 ± 1.0 mV, indicating the presence of cationic amine groups of chitosan on the particle surface. Subsequently, liposomes consisting of hydrogenated L-α-phosphatidylcholine (Egg PC) and cholesterol (50:50 weight ratio) were prepared by vesicle extrusion technique. In order to exclude the interference of ionic strength in surface ζ potential measurements, the liposomes were prepared in deionized water. The size and surface ζ potential of the formed liposomes were 110 ± 1 nm and −14.1 ± 0.4 mV, respectively (Figure 2C). Then the AuChi-liposome were prepared by mixing the synthesized liposomes and AuChi at a molar ratio of 1:300 under gentle

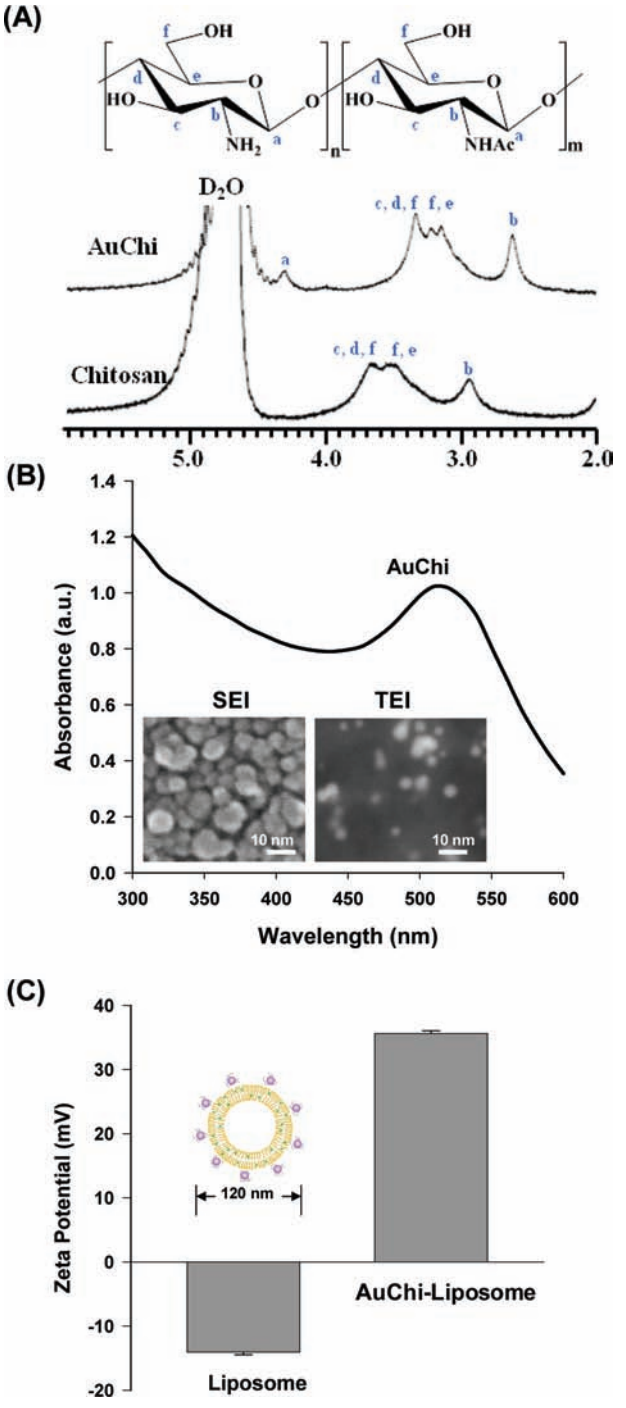

Figure 2. Synthesis and characterization of AuChi and AuChi-liposome. (A) ^{1}H NMR spectra of chitosan and AuChi, indicating the coating of chitosan on the surface of gold nanoparticles. (B) UV−vis absorption spectrum of AuChi. Insets: representative secondary electron image (SEI) of AuChi and transmitted electron image (TEI) of the inner gold nanoparticles of AuChi. (C) The surface ζ potential (mV) of bare liposome (without AuChi) and AuChi-liposome with a liposome/AuChi molar ratio of 1:300.

dx.doi.org/10.1021/ja111110e |J. Am. Chem. Soc. 2011, 133, 4132–4139

bath sonication for 10 min. The size and surface ζ potential of the resulting AuChi-liposome complexes were characterized by DLS. The measured size of AuChi-liposome was slightly larger than that of bare liposomes, suggesting the adsorption of 10 nm AuChi onto the liposome surface. The surface ζ potential changed explicitly from −14.1 ± 0.4 to 35.6 ± 0.4 mV (Figure 2C), which confirms the binding of positively charged AuChi to the negatively charged liposomes through electrostatic attraction.

The stability of AuChi-liposome was evaluated by a fluorescence assay consisting of 8-aminonaphthalene-1,3,6-trisulfonic acid disodium salt (ANTS) and *p*-xylene-bis-pyridinium bromide (DPX). ANTS is a polyanionic fluorophore, and DPX is a corresponding cationic quencher. This pair of fluorophore/quencher has been widely used to study liposomal leakage upon liposome fusion with one another or with other biological membranes and thus to evaluate the stability of liposomes.[33,34] When these two dyes are coencapsulated inside liposomes at a proper molar ratio, the fluorescence emission of ANTS can be maximally quenched by DPX through a collisional quenching effect. However, when the dye-loaded liposomes are not stable and fuse with other substances, the dyes will leach out of the liposomes and be diluted by the surrounding medium. The dilution will reduce the chance of collision between ANTS and DPX and then lead to fluorescence recovery of ANTS. Therefore, with an excitation at 360 nm, ANTS emission signal at 510 nm is typically used to test the stability of liposomes. For instance, Figure 3A shows the fluorescence emission signal of ANTS/DPX-loaded liposomes in PBS and in the presence of 1% Triton X-100 surfactant, respectively. It was clearly seen that negligible signal from ANTS was detected when the liposomes were intact in PBS buffer, but a significant signal increase occurred in the presence of a membrane pore-forming surfactant, such as Triton X-100. Herein we tested the stability of the AuChi-liposome complex at various liposome/AuChi molar ratios (e.g., 1:0, 1:150, and 1:300). The AuChi-liposome were preloaded with ANTS and DPX, and then each sample was incubated with bare liposomes at the molar ratio of 1:4 for 1 h. The bare liposomes were neither stabilized with AuChi nor loaded with the dye pair. If fusion between AuChi-liposome and bare liposomes occurs, then it is expected that some of the dyes will transfer from AuChi-liposome to bare liposomes. To amplify the signal of the transferred dyes, the sample was centrifuged through a filter membrane at 13.2×10^3 rpm for 20 min, at which condition both bare liposomes and unstable AuChi-liposome were ruptured and completely released the dyes, while stable AuChi-liposome remained intact. Therefore, the fluorescence intensity of ANTS detected in the filtrate was the accumulative signal from unstable AuChi-liposome that have fused with either bare liposomes or filter membrane. As shown in Figure 3B, a high level of ANTS signal was detected when the liposomes were not protected by any AuChi. In contrast, when the liposome/AuChi molar ratio was 1:150 and 1:300, the detected ANTS signal was only 30 and 20%, respectively, of the bare liposomes. The obtained ANTS signal at low liposome/AuChi molar ratios (e.g., 1:150 and 1:300) may be attributed to incomplete quenching of ANTS by DPX. The collisional quenching mechanism of this pair of dyes determines that the fluorescence quenching is neither permanent nor complete. These results demonstrate that the adsorption of AuChi on liposome surface can effectively prevent them from fusing with one another or filter membranes under vigorous centrifugation and thus significantly improve the

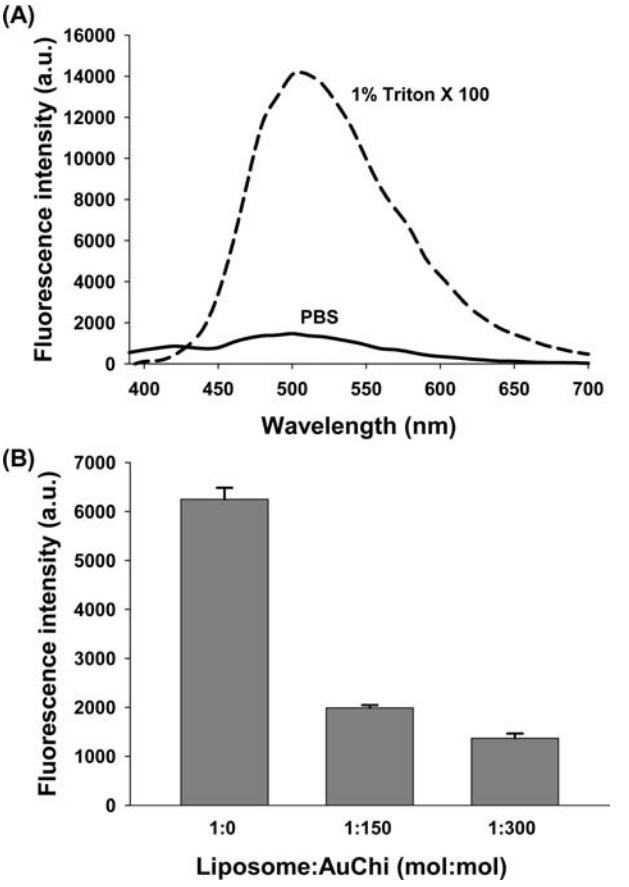

Figure 3. Fusion ability of AuChi-liposome at different liposome/AuChi molar ratios. The fluorescent dyes, ANTS and DPX, were encapsulated inside the liposomes at a concentration that DPX maximally quenched the fluorescence of ANTS. Upon fusion with bare liposomes (without AuChi or dyes), the fluorescence of ANTS recovered due to the dilution of the dyes. (A) The measured fluorescence emission spectra of ANTS after incubating ANTS/DPX-loaded liposomes in PBS (serving as background fluorescence signal) and in 1% Triton X-100 (serving as maximal fluorescence signal), respectively, for 1 h at room temperature. (B) AuChi-liposome with a liposome/AuChi molar ratio of 1:0, 1:150, or 1:300 were mixed with bare liposomes (without AuChi or dyes) at a molar ratio of 1:4. After incubation for 1 h at room temperature, the bare liposomes were broken by fusing with a centrifugal filter unit. The resulting fluorescence emission intensity of ANTS in the filtrate at 510 nm was measured.

stability of the liposomes. These results are also consistent with a previous stability study using negatively charged carboxyl-modified gold nanoparticle to stabilize cationic liposomes.[30] As a liposome/AuChi molar ratio of 1:300 gave the most stable formulation, we selected this formulation for the subsequent toxin-triggered drug release studies.

With the liposome/AuChi molar ratio fixed, the liposome formulation was further optimized to obtain the highest pore-forming property by bacterial toxin, α-toxin in particular. The α-toxin is one of the pore-forming toxins secreted by *S. aureus* bacterium and also is the most commonly reported toxin to form pores in artificial or biological membranes.[13] To find an optimal liposome formulation that is the most sensitive to α-toxin, two parameters were investigated: the content of cholesterol in liposome membranes and the addition of PEG to the liposome solutions. Both parameters have been previously reported to

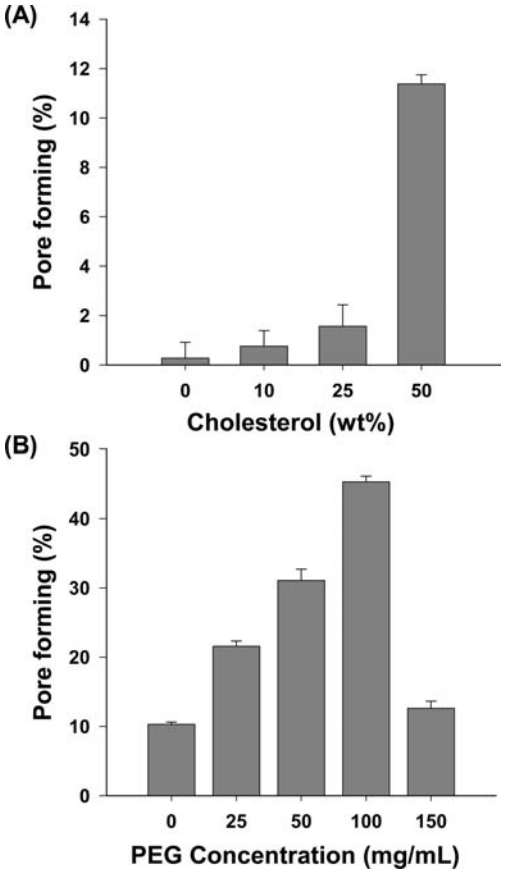

Figure 4. Toxin-induced pore forming in liposome membranes at various concentrations of cholesterol and PEG. (A) Liposomes with 0, 10, 25, and 50% (w/w) cholesterol were incubated with 20 μg/mL α-toxin for 1 h at room temperature. The dyes released from the pores were quantified by measuring fluorescence emission intensity of ANTS at 510 nm. Percentage of pore forming was obtained by comparing the α-toxin induced dye release with complete dye release caused by 1% (v/v) Triton-X-100. (B) Liposomes with 50% (w/w) cholesterol were incubated with 20 μg/mL α-toxin for 1 h at room temperature in the presence of various concentrations of PEG molecules (M_n = 2000 Da), ranging from 0 to 150 mg/mL.

affect the pore-forming activity of toxins in artificial membranes.[35−37] In this study, ANTS/DPX dyes containing liposomes with different cholesterol levels (e.g., 0, 10, 25, and 50 wt %) were prepared and then incubated with α-toxin (20 μg/mL) for 1 h prior to measuring the fluorescence emission of ANTS. Maximal dye leakage was obtained by lysing all liposomes with 1% (v/v) Triton X-100, while fluorescence emission of the dyes from corresponding liposomes in PBS served as a background signal. Percentage of pore forming by α-toxin was calculated using the formula: Percentage of pore forming (%) = $(I_{\alpha\text{-toxin}} - I_{PBS})/(I_{TX\text{-}100} - I_{PBS}) \times 100$, in which $I_{\alpha\text{-toxin}}$, I_{PBS}, and $I_{TX\text{-}100}$ represent fluorescence emission intensity at 510 nm of the liposome formulations incubated with α-toxin, PBS, and Triton-X-100, respectively. As shown in Figure 4A, an increase in pore forming was observed when cholesterol content increased, suggesting that cholesterol augments the pore-forming efficiency of α-toxin. It was found that 50 wt % of cholesterol in the liposome membrane allowed maximal pore-forming activity of α-toxin. It has been hypothesized that cholesterol can promote the interaction between α-toxin and phosphatidylcholine

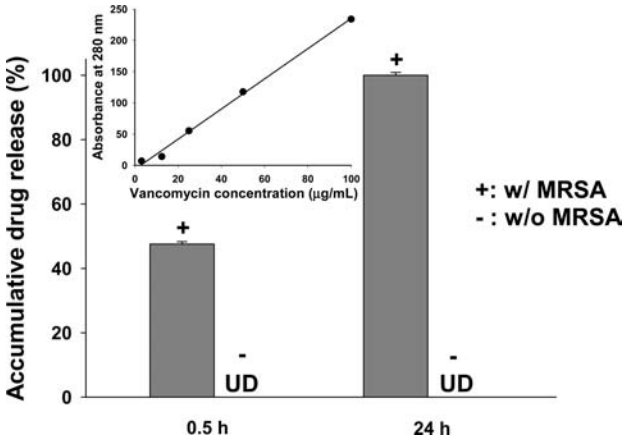

Figure 5. Accumulative vancomycin release profile from vancomycin-loaded AuChi-liposome after incubation with MRSA bacteria (1×10^8 CFU/mL) for 0.5 and 24 h, respectively. The released vancomycin was quantified by reversed phase HPLC. The corresponding samples incubated with PBS (without MRSA bacteria) were used as negative controls. Inset: the linear calibration standard curve of vancomycin at various concentrations measured by HPLC.

headgroup[37] or interact with α-toxin itself.[36] Next we fixed the cholesterol concentration at 50 wt % in the liposome formulation and investigated the effects of PEG on the pore-forming activity of α-toxin. ANTS/DPX-containing liposomes were first mixed with PEG at different PEG concentrations ranging from 0 to 150 mg/mL and then incubated with α-toxin for 1 h, followed by quantifying the percentage of pore forming. As shown in Figure 4B, when PEG concentration in the solution increased from 0 to 100 mg/mL, pore forming increased and then reached the maximum at 100 mg/mL. However, the pore forming dropped when the PEG concentration was higher than 100 mg/mL. The role of PEG is to dehydrate liposome surfaces because of its strong hydrogen bonding with water and thus to facilitate the membrane insertion process of toxins.[35] These results suggest that the most sensitive liposome formulation to α-toxin contains 50% cholesterol in the liposome membrane and 100 mg/mL PEG in the solution.

Once the toxins insert into the membrane, the assembled protein oligomers are stable over a wide range of pH and temperature, and the formed transmembrane pores stay open at normal conditions. Through these pores, drug payloads can be released from the liposomes. In order to verify our hypothesis of using toxins to form pores and trigger the release of drugs from AuChi-liposome, we chose MRSA as a bacterium model that secretes toxins and vancomycin as an antibiotic model that has strong inhibitory effects against MRSA bacteria. In the study, optimal formulation of AuChi-liposome determined from the above studies were loaded with 10 mg/mL of vancomycin and incubated with MRSA252 bacteria (1×10^8 CFU/mL) in 5% TSB at 37 °C. At predetermined time points, released vancomycin was collected from the mixture solution using a centrifugal filter unit with a molecular weight cutoff of 100 KDa. The concentration of vancomycin was determined by reversed phase HPLC. In the experiment, the final vancomycin concentration was about 62 μg/mL. As the minimal inhibitory concentration (MIC) of vancomycin against MRSA bacteria is about 2 μg/mL,[38] we hypothesize that the amount of vancomycin absorbed by cell membranes will not significantly affect the measurement

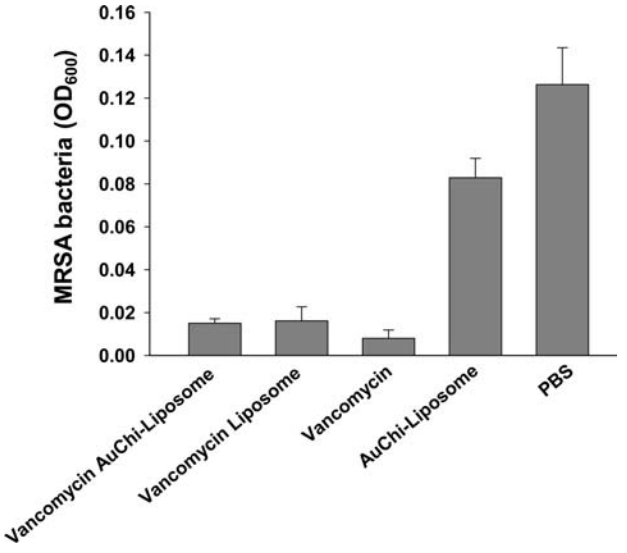

Figure 6. Antimicrobial activity of vancomycin AuChi-liposome against MRSA bacteria. Vancomycin AuChi-liposome were incubated with MRSA bacteria (1×10^8 CFU/mL) in 5% TSB for 24 h in the presence of 100 mg/mL PEG. The toxins secreted by the bacteria form pores in the AuChi-liposome and release the encapsulated vancomycin, which subsequently inhibits the growth of the bacteria. The bacterial growth rate was determined by measuring absorbance at 600 nm after incubation. Vancomycin liposome (without AuChi) and free vancomycin with the same drug concentration (62 μg/mL) served as positive controls. AuChi-liposome (without vancomycin) and PBS served as negative controls. Data represent mean ± SD ($n = 3$).

of vancomycin release kinetics. In the study, we first measured the UV absorbance intensity at 280 nm of a series of vancomycin samples ranging from 0 to 100 μg/mL to generate a standard curve (Figure 5, inset). Then the concentration of the released vancomycin was quantified by comparing the measured absorbance intensity with the standard curve. As shown in Figure 5, at 0.5 and 24 h post incubation of vancomycin-loaded AuChi-liposome with MRSA bacteria, 29.5 and 62.0 μg/mL of vancomycin were detected in the release medium, which translates to accumulative drug release of 48 and 100% of the total encapsulated vancomycin, respectively. In contrast, no free vancomycin was detected at either time point when the vancomycin-loaded AuChi-liposome were incubated in the absence of MRSA bacteria. This further confirms that AuChi-liposome remained stable during the centrifugation process, and thus the vancomycin detected in the presence of MRSA was solely contributed by the bacterial toxins through forming pores on liposome membranes. Since 24 h is a standard incubation time to study antimicrobial activity of antibiotics, complete drug release from vancomycin-loaded AuChi-liposome obtained at this time point implies the potential application of this system to efficiently suppress bacterial growth.

After having demonstrated the drug release from AuChi-liposome in the presence of toxins secreted by MRSA bacteria, we further examined the ability of vancomycin-loaded AuChi-liposome to inhibit the growth of MRSA252 in vitro. Vancomycin-loaded AuChi-liposome were incubated with MRSA252 (1×10^8 CFU/mL) in 5% TSB for 24 h, followed by OD_{600} measurement to determine the bacterial growth. Vancomycin-loaded liposomes without AuChi stabilization and free vancomycin were used as positive controls; blank AuChi-liposome (without vancomycin) and PBS served as negative controls. As shown in Figure 6, vancomycin AuChi-liposome were able to inhibit the growth of MRSA252 to the same extent as vancomycin liposome and free vancomycin. The student t test showed that the difference between the OD_{600} value of vancomycin AuChi-liposome and that of vancomycin were insignificant with a p-value of 0.18 ($p > 0.1$). The obtained OD_{600} signal of vancomycin AuChi-liposome has been subtracted by that of AuChi-liposome (without vancomycin) to exclude any possible interference signal from the bare liposomal drug carriers. The observed non-negligible inhibitory effects of AuChi-liposome in Figure 6 might be due to some intrinsic properties of lipids and/or the interactions between unbound AuChi nanoparticles and the bacteria. Although both vancomycin AuChi-liposome and vancomycin liposome inhibited the growth of MRSA252 bacteria, their working mechanisms were different. Vancomycin AuChi-liposome were stabilized against fusion and did not release drugs in the absence of bacterial toxins. Thus, their observed inhibitory effect was merely due to the released vancomycin through the pores formed by bacterial toxins. In contrast, vancomycin liposome was not protected by AuChi and could readily fuse with each other and bacterial membranes resulting in vacomycin release, which answered for the observed inhibitory effect. Comparing to bare vancomycin liposome, the vancomycin AuChi-liposome system exhibits several distinct advantages. First, it improves the shelf-time of the liposome formulation that minimal amounts of drugs will be released prior to administration. Second, it enables bacteria-targeted antibiotic delivery. As this formulation does not fuse with biological membranes, the drugs will only be released at the infectious sites where the bacteria secrete toxins. Lastly, the dosage of the antibiotics is self-regulated by the severeness of the infections. More bacteria will secrete more toxins and thus trigger more drug release. Note that the MIC of vancomycin against MRSA is about 2 μg/mL.[38] The released vancomycin from vancomycin AuChi-liposome had a concentration up to 62 μg/mL, which should be sufficient to inhibit the growth of the bacteria.

CONCLUSIONS

In conclusion, a novel passive targeting antimicrobial drug delivery platform was developed, in which bacterial toxins were utilized to trigger antibiotic release from gold nanoparticle-stabilized liposomes for inhibiting the growth of the toxin-secreting bacteria. We systematically optimized the liposome composition and the coverage of chitosan-modified gold nanoparticles on the liposome surface so that the liposome fusion activity and the undesirable drug leakage were prohibited at normal storage conditions, while the liposomes were still susceptible to pore-forming toxins. Once incubated with toxins, the liposomes became leaky, and the encapsulated antibiotic payloads were rapidly released through the toxin-formed pores. We further demonstrated that in the presence of toxin-secreting bacteria, 100% of the encapsulated antibiotics were released from the gold nanoparticle-stabilized liposomes, and bacterial growth was effectively inhibited by the released antibiotics in 24 h. This antimicrobial drug delivery approach provides an entirely new paradigm for the treatment of bacterial infections by specifically releasing drugs at the infectious sites, while minimizing possible off-target effects. While vancomycin was used as an anti-MRSA antibiotic in this study, this technique can be generalized to

deliver a variety of antimicrobials and antibiotics for the treatment of various infections caused by bacteria or other organisms that secrete pore-forming proteins.

AUTHOR INFORMATION

Corresponding Author
zhang@ucsd.edu

ACKNOWLEDGMENT

This work is supported by the University of California San Diego (faculty startup funds and a faculty career development award) and partially by the National Science Foundation grant CMMI-1031239 and the National Institute of Health grants R01AI067395-01 and 1R21AI088147-01A1.

REFERENCES

(1) Liu, R.; Kay, B. K.; Jiang, S.; Chen, S. *MRS Bull.* **2009**, *34*, 432–440.
(2) Wang, A. Z.; Gu, F.; Zhang, L.; Chan, J. M.; Radovic-Moreno, A.; Shaikh, M. R.; Farokhzad, O. C. *Expert Opin. Biol. Ther.* **2008**, *8*, 1063–1070.
(3) Langer, R. *Nature* **1998**, *392* (SUPP), 5–10.
(4) Davis, M. E.; Chen, Z. G.; Shin, D. M. *Nat. Rev. Drug Discovery* **2008**, *7*, 771–782.
(5) Farokhzad, O. C.; Cheng, J.; Teply, B. A.; Sherifi, I.; Jon, S.; Kantoff, P. W.; Richie, J. P.; Langer, R. *Proc. Natl. Acad. Sci. U.S.A.* **2006**, *103*, 6315–6320.
(6) Shen, X.; Valencia, C. A.; Szostak, J. W.; Dong, B.; Liu, R. *Proc. Natl. Acad. Sci. U.S.A.* **2005**, *102*, 5969–5974.
(7) Hu, C. M.; Kaushal, S.; Tran Cao, H. S.; Aryal, S.; Sartor, M.; Esener, S.; Bouvet, M.; Zhang, L. *Mol. Pharmaceutics* **2010**, *7*, 914–920.
(8) Shi, J.; Votruba, A. R.; Farokhzad, O. C.; Langer, R. *Nano Lett.* **2010**, *10*, 3223–3230.
(9) Okumus, B.; Arslan, S.; Fengler, S. M.; Myong, S.; Ha, T. *J. Am. Chem. Soc.* **2009**, *131*, 14844–14849.
(10) Vecsey-Semjen, B.; Kwak, Y. K.; Hogbom, M.; Mollby, R. *J. Membr. Biol.* **2010**, *234*, 171–181.
(11) Xu, D.; Cheng, Q. *J. Am. Chem. Soc.* **2002**, *124*, 14314–14315.
(12) Yu, Y.; Vroman, J. A.; Bae, S. C.; Granick, S. *J. Am. Chem. Soc.* **2010**, *132*, 195–201.
(13) Bhakdi, S.; Tranum-Jensen, J. *Microbiol. Rev.* **1991**, *55*, 733–751.
(14) Song, L.; Hobaugh, M. R.; Shustak, C.; Cheley, S.; Bayley, H.; Gouaux, J. E. *Science* **1996**, *274*, 1859–1866.
(15) Meesters, C.; Brack, A.; Hellmann, N.; Decker, H. *Proteins* **2009**, *75*, 118–126.
(16) Zhang, L.; Pornpattananangkul, D.; Hu, C.-M. J.; Huang, C.-M. *Curr. Med. Chem.* **2010**, *17*, 585–594.
(17) Castro, G. A.; Ferreira, L. A. *Expert Opin. Drug Delivery* **2008**, *5*, 665–679.
(18) Kim, H. J.; Jones, M. N. *J. Liposome Res.* **2004**, *14*, 123–139.
(19) Stockler, S.; Lackner, H.; Ginter, G.; Schwinger, W.; Plecko, B.; Muller, W. *Eur. J. Pediatr.* **1993**, *152*, 981–983.
(20) Walsh, T. J.; Goodman, J. L.; Pappas, P.; Bekersky, I.; Buell, D. N.; Roden, M.; Barrett, J.; Anaissie, E. J. *Antimicrob. Agents Chemother.* **2001**, *45*, 3487–3496.
(21) Haluska, C. K.; Riske, K. A.; Marchi-Artzner, V.; Lehn, J.-M.; Lipowsky, R.; Dimova, R. *Proc. Natl. Acad. Sci. U.S.A.* **2006**, *103*, 15841–15846.
(22) Lei, G.; MacDonald, R. C. *Biophys. J.* **2003**, *85*, 1585–1599.
(23) Marrink, S.; Mark, A. E. *J. Am. Chem. Soc.* **2003**, *125*, 11144–11145.
(24) Moghimi, S. M.; Szebeni, J. *Prog. Lipid Res.* **2003**, *42*, 463–478.
(25) Woodle, M. C. *Adv. Drug Delivery Rev.* **1998**, *32*, 139–152.
(26) Zhang, L.; Gu, F. X.; Chan, J. M.; Wang, A. Z.; Langer, R. S.; Farokhzad, O. C. *Clin. Pharmacol. Ther.* **2008**, *83*, 761–769.
(27) Wang, B.; Zhang, L.; Bae, S. C.; Granick, S. *Proc. Natl. Acad. Sci. U.S.A.* **2008**, *105*, 18171–18175.
(28) Yu, Y.; Anthony, S. M.; Zhang, L.; Bae, S. C.; Granick, S. *J. Phys. Chem. C* **2007**, *111*, 8233–8236.
(29) Zhang, L.; Granick, S. *Nano Lett.* **2006**, *6*, 694–698.
(30) Pornpattananangkul, D.; Olson, S.; Aryal, S.; Sartor, M.; Huang, C. M.; Vecchio, K.; Zhang, L. *ACS Nano* **2010**, *4*, 1935–1942.
(31) Aryal, S.; B, K. C. R.; Dharmaraj, N.; Bhattarai, N.; Kim, C. H.; Kim, H. Y. *Spectrochim. Acta, Part A* **2006**, *63*, 160–163.
(32) Yang, D.; Pornpattananangkul, D.; Nakatsuji, T.; Chan, M.; Carson, D.; Huang, C. M.; Zhang, L. *Biomaterials* **2009**, *30*, 6035–6040.
(33) Blackwood, R. A.; Smolen, J. E.; Hessler, R. J.; Harsh, D. M.; Transue, A. *Biochem. J.* **1996**, *314* (Pt 2), 469–475.
(34) Wyman, T. B.; Nicol, F.; Zelphati, O.; Scaria, P. V.; Plank, C.; Szoka, F. C. *Biochemistry* **1997**, *36*, 3008–3017.
(35) Bashford, C. L.; Alder, G. M.; Fulford, L. G.; Korchev, Y. E.; Kovacs, E.; MacKinnon, A.; Pederzolli, C.; Pasternak, C. A. *J. Membr. Biol.* **1996**, *150*, 37–45.
(36) Forti, S.; Menestrina, G. *Eur. J. Biochem.* **1989**, *181*, 767–773.
(37) Watanabe, M.; Tomita, T.; Yasuda, T. *Biochim. Biophys. Acta* **1987**, *898*, 257–265.
(38) Sakoulas, G.; Moise-Broder, P. A.; Schentag, J.; Forrest, A.; Moellering, R. C., Jr.; Eliopoulos, G. M. *J. Clin. Microbiol.* **2004**, *42*, 2398–2402.